2003

Effect of iron and iron/yttrium codoping on the densification of a-alumina

Michael David Drahus
Lehigh University

Drahus, Michael David

Effect of Iron and Iron/Yttrium Codoping on the Densification of a-Alumina

January 2004

Effect Of Iron and Iron/Yttrium Codoping On the Densification Of α-Alumina

By
Michael David Drahus

A Thesis
Presented to the Graduate and Research Committee
of Lehigh University
In Candidacy for the Degree of
Master of Science

in
Materials Science and Engineering

Lehigh University
January 2004

Certificate Of Approval

This thesis is accepted and approved in partial fulfillment of the requirements for the Master of Science.

12-8-03
Date

Thesis Advisor

Co-Advisor

Chairperson of Department

ACKNOWLEDGMENTS

I would like to extend my gratitude to everyone that has helped make my stay at Lehigh University a productive one. In particular, my advisor, Dr. Martin P. Harmer, whose patience I am sure I have tested on more than one occasion. Also my coadvisor, Dr. Helen M. Chan, for enduring my proclivity for appearing at her office door for impromptu discussions of data...usually when she is applying herself to a task from which she would rather not be disturbed. Dr.'s Donald M. Smyth and Andrey N. Suokhojak were also very helpful in their willingness to share their knowledge of defect chemistry, experimental methods and data interpretation. Dr. Donna Narsavage, formally of the University Of Scranton, whose experience with experimental methods and chemistry saved me a lot of frustration.

The advice and instruction offered by the research technicians were also invaluable. Many thanks to Gene Kozma, Mike Rex, Dave Ackland (whistler extraordinaire), William Mushock, Guy Faylor and of course, Arlan Benscoter. Recognition must also be given to the secretaries for keeping me administratively correct... Maxine Mattie (The REAL boss of the department), Virginia Newhard, Deanne Hoenscheid and Sue Stetler.

I would like to thank my fellow graduate students in the ceramics research group for their help with equipment questions. Also Rick Noecker and Ryan Deacon for their help when software would misbehave, enjoyable discussions of topics both academic and nonacademic and for just being good fellows.

In the extracurricular area, I would like to thank Big Joe, Slappy, Brian, Mike, Mary Heather, Stephanie and all the other fellows and ladies that frequent the B.K.S. Good company and the late evening workouts on the speed bag, heavy bag and weights were priceless in their ability to relieve the stress of the day.

I would also like to thank my sister, Dr. Barbara Worden, for her efforts in enlightening me to the workings of the world of academia, how it differs from a construction site and why "You can't just go and do things that way there". Her advice in these matters through out the years has been both beneficial and welcome.

Finally, I would like to thank the people without whom all this would not be possible...my Mother and Father. Through out my life you never stopped believing in me even when I suffered the most damaging setbacks. Mother, I am happy that you are still with us to see this graduation. Father, you are with us in our memories and in spirit. Be assured I am in no way finished yet...there are still many challenges left to conquer.

Onward to meet them.

Table of Contents

List of Figures

Abstract

The effect of iron and iron/yttrium codoping on the densification of ultra high-purity, (99.995%) fine grained alumina has been studied under both oxidizing and reducing conditions. Addition of 1000ppm Fe under oxidizing conditions was found to reduce the densification rate by a factor of 5 and also retard the grain growth rate. In a nitrogen atmosphere (Po_2 ~3.2×10^{-4} atm.), the densification rate was similar to the undoped samples. Further reducing the Po_2 (to 5.1×10^{-14} atm.) in an N_2/H_2 atmosphere caused a continued increase of the densification rate to 2.5 orders of magnitude over that of the undoped samples.

In the codoped samples containing 1000/1000 ppm iron/yttrium there was no detectable difference in the densification rate between the samples prepared under oxidizing conditions and those prepared in the nitrogen atmosphere. However, in the samples prepared in the N_2/H_2 atmosphere the presence of the Fe^{+2} negated the effect of the yttrium and raised the densification rate of the codoped samples to that of the undoped material.

1. Introduction and Background

1.1 Introduction

Previous work in the 1970's examined the effect of iron doping on the creep and densification rate of alumina [1-3]. The results of these experiments yielded the following conclusions:

1) The creep and densification rates were dependent on atmosphere.
2) Fe^{+2} and Fe^{+3} enhance the densification and creep rate.
3) Fe^{+2} enhances the creep and densification rate more than Fe^{+3}.

The increase in rate processes under reducing conditions was explained by a defect chemistry argument where the presence of Fe^{+2} increased the concentration of aluminum interstitial ions, $Al_i^{\cdots}$. However, there was no postulation made as to why iron under oxidizing conditions enhanced the densification rate of alumina.

Recent work at Lehigh University examining the effects of transition metals both in singly and in codoped combinations on the creep of alumina has found some inconsistencies with the previous work. It has been observed that the addition of 100ppm iron to alumina produces a decrease in the creep rate ranging from a factor of between 10 to 5 over the temperature interval of 1200°C and 1350°C respectively for 100ppm Fe doped alumina tested in air (Figure 1). It is a reasonable expectation that, since densification and creep are related processes, when a change in the creep rate under a given set of experimental conditions is observed, a corresponding change in the densification rate under the same conditions will also be observed.

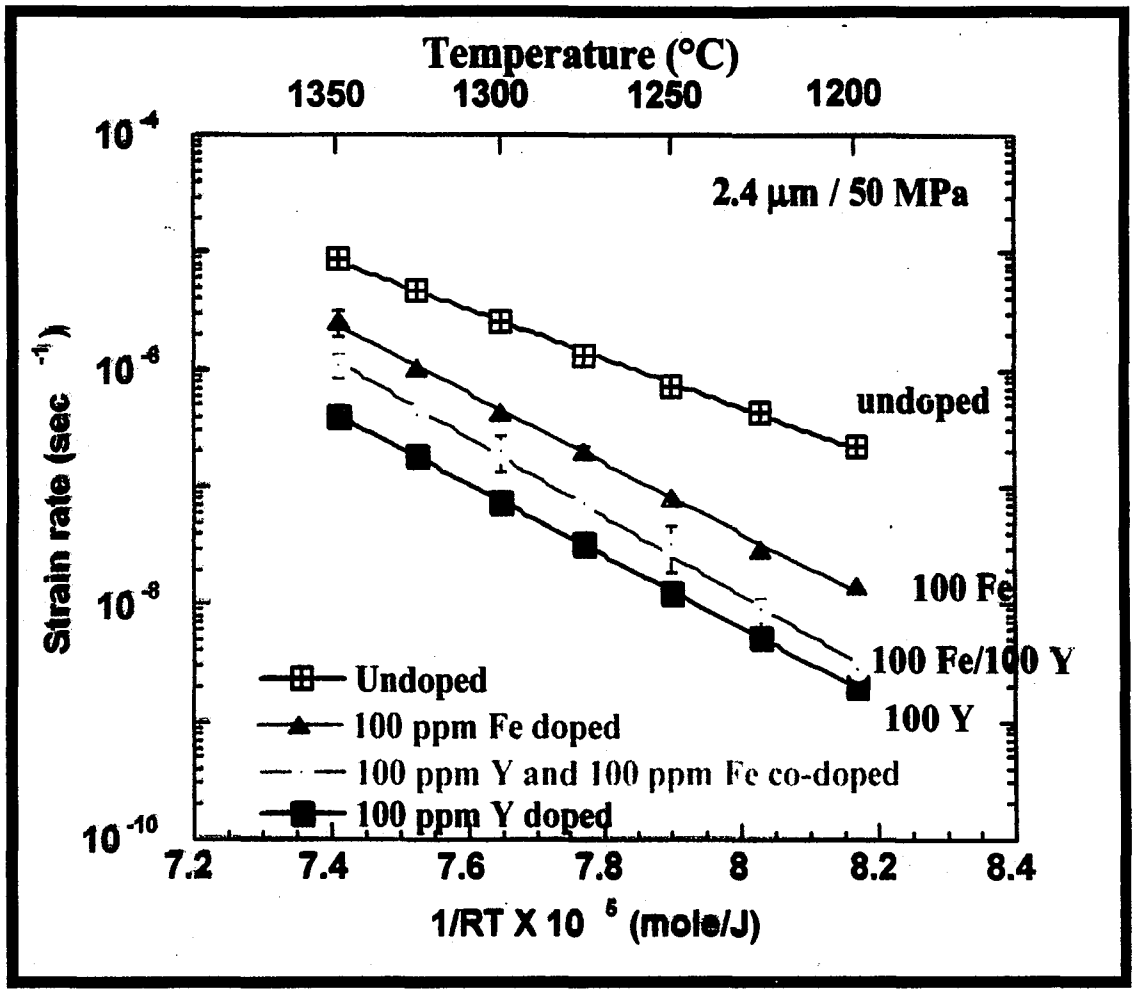

Figure 1. Strain Rate vs Temperature under oxidizing conditions for 100ppm singly and codoped fine grained alumina ranging from 1200°C to 1350°C. Courtesy C.Wang.

The purpose of this study is to examine the effect of iron and iron/yttrium codoping on the densification of fine grained alumina and to correlate the results with recent creep data acquired under similar experimental conditions. The previous [1-3] densification and creep work was conducted at larger grain sizes, higher temperatures and higher dopant concentrations. Under the differing conditions, it is not unreasonable to postulate that a change in the rate controlling mechanism and species may reveal itself.

1.2 Background

The results of Rao and Cutler [1] indicated that under oxidizing conditions, the volume diffusion coefficient increased in proportion to the concentration of iron , figure 2.

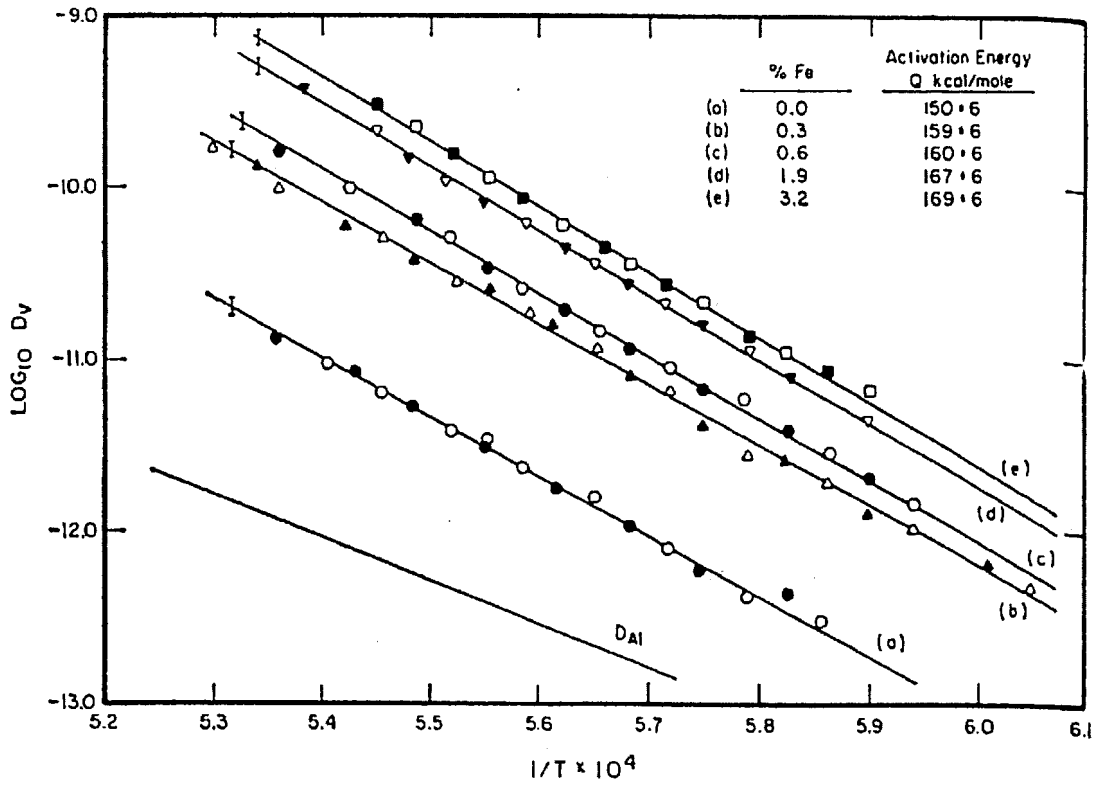

Figure 2. Volume diffusion coefficient for Fe-doped Al_2O_3 spheres in air in the temperature range of 1630°C to 1880°C.

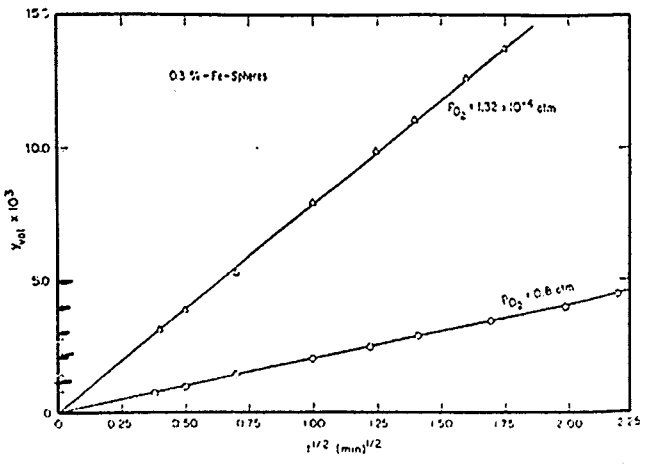

Figure 3. Isothermal shrinkage data for 9μ 0.3 % Fe-doped spheres showing Po_2 dependence of sintering rate at 1480°C

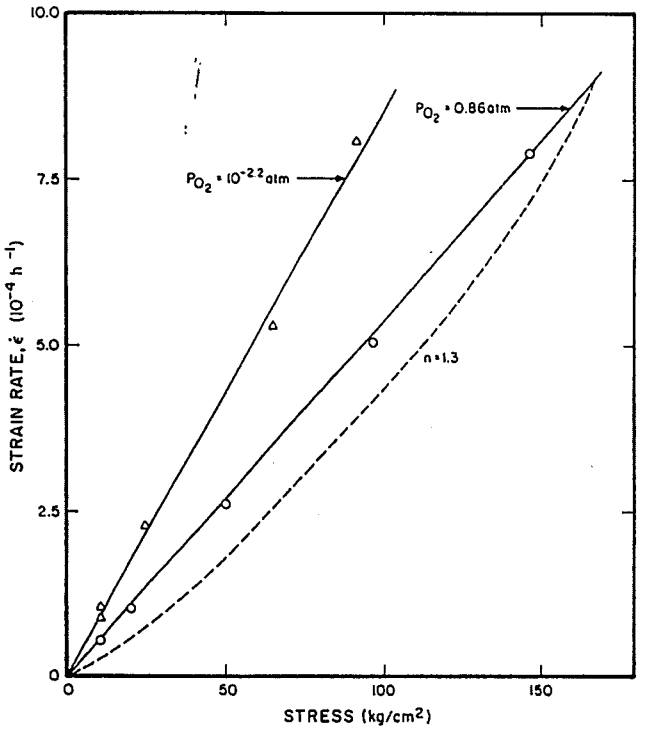

Figure 4. Linear plot of stress vs. strain rate for polycrystalline Al_2O_3 doped with 1% Fe (10μ) and creep tested at 1500°C

It was also determined that the densification rate was inversely proportional to the oxygen partial pressure (Figure 3). The work of Hollenburg and Gordon on creep found similar results (figure 4).

The increase in both the densification and creep rate under reduced oxygen partial pressure has been attributed to a classic defect chemistry effect where the compensating point defect is the aluminum cation interstitial.

$$Fe_{Al}^{x} \Leftrightarrow 3Fe_{Al}^{'} + Al_i^{\bullet\bullet\bullet}$$

This conclusion was also drawn by by both Rao and Cutler and Hollenburg and Gordon [1,2].

In a review of the creep, densification and electrical properties measurements of several researchers, Dutt and Kroger [4] proposed a defect model involving $Fe_{Al}^{'}$ and $Al_i^{\cdots}$ as the dominant compensating ionic defects to describe the effect of Po_2 and temperature on the transport rate. All previous work seems to be in agreement that the presence of Fe^{+2} enhances the lattice diffusion of Al^{+3}. The grain boundary diffusion coefficient of the Al^{+3} cation was also observed to increase [5] and an increase in the grain boundary diffusion coefficient of oxygen has been mentioned [3].

There are three experimental parameters that differ between the Lehigh creep study and the work of Rao and Cutler and Hollenburg and Gordon [1,2] that need to be highlighted : the grain size, the temperature and dopant level .

The grain sizes of the samples used by Rao and Cutler and Hollenburg and Gordon [1,2] were in the range of 15 μm to 20μm and 10μ respectively compared to the 1-2μ grain size used in the Lehigh study. The grain sizes in the two experiments differ by a factor of up to 20 and, using the relation applied by Laurent and Benard [6], this corresponds to a 73 fold increase in grain boundary transport relative to lattice transport at the finer grain size.

The temperature difference also needs to be considered. The majority of the previous experiments conducted on creep and densification were carried out at much higher temperatures (ranging from 1450 to 1900°C) than in the present study (between 1200 and 1350°C). In general, bulk diffusion normally has a higher activation energy than the grain boundary diffusion [7], and one would expect it to play a larger role at higher temperatures. Also, the ability of the lattice to accommodate oversized dopant atoms is proportional to the temperature. The dopant concentrations used in the previous creep and

densification studies [1,2,3,5,8] were much higher (up to 320 times higher) than the present creep study.

The smaller grain sizes, lower temperatures and lower dopant levels of the Lehigh creep study favor grain boundary diffusion over volume diffusion. Work done by Berry, Zhao and Harmer [9,10] on fine grained alumina showed that the rate controlling mechanism was grain boundary diffusion even at temperatures of 1600°C.

Yttrium is effective in reducing the densification and creep rate in alumina[11-14]. Due to its low solubility in alumina , ~10ppm[15], it preferentially segregates to the grain boundaries [16,17]. The effect of yttrium (and other dopants that segregate to the grain boundaries) has been attributed to its ability to block the diffusion paths of the cations or anions in the grain boundary and thus hinder the diffusion process [17]. The large size of the dopant causes a strain in the lattice as a substitutional cation. Elsasser and Fabris have calculated the lattice strain associated with oversized dopant atoms of the B III group [19]. Both Y^{+3} (0.89 Å) and Fe^{+3} (0.65 Å) are larger than Al^{+3} (0.53Å) and, therefore, by size alone, one would expect yttrium to have a greater effect at inhibiting the diffusion in the grain boundaries.

There are also electronic interactions to be considered. Prott and Le Gall [15] found that the presence of Yttrium in the grain boundaries caused a decrease in the oxygen grain boundary diffusion coefficient. Elsasser and Marinopoulos [19] modeled the segregation of yttrium and other cations to more ordered boundaries where both the Al cation and the dopant were in an octahedral coordination. They found that there was an overlap of the yttrium 4p orbitals with the oxygen 2s orbitals.

This overlap caused the Y-O bond to take on more of a covalent character and increase the electron density along the bond axis.

It has been found that yttrium has the ability to influence the bonding of the aluminum cation. The disorder that exists in the grain boundaries allows the cations of both the dopant(s) and host material to be coordinated by the oxygen anions in configurations other than octahedral. Modeling, electronic band structure calculations and electron energy loss spectroscopy conducted on grain boundaries in α-alumina have concluded that some of the aluminum cations can exist in a tetrahedral coordination [20-22]. In the Y-Al-O system, tetrahedral coordination for the Al cation, $Al_{tet,}$ is found in the compounds $Y_3Al_5O_{12}$ (YAG) and $Y_4Al_2O_9$ (YAM). Band structure calculations conducted on these systems by Ching and Xu[24] showed that, in the case of $Al_{tet,}$ the Al-O bond has a shorter bond length than in a the α-alumina crystal structure and thus is stronger. Charge density and local density of states calculations also showed that an Al_{tet} in YAG and YAM has the ability to interact with the yttrium cation whereas Al_{oct} is shielded by the neighboring oxygens in a manner that curtails this phenomenon. This bonding between Y and Al_{tet} limits the movement of the Al cation and manifests itself in a reduction of the rate processes relative to undoped α-alumina when this atomic configuration is present.

From these studies, it can be seen that yttrium, in the disordered region of a grain boundary, has the ability to interact with both the oxygen anion and the aluminum cation in a manner that hinders the diffusion of both.

In contrast to the wealth of theoretical information available concerning the bonding in the Y-Al-O system, experimental studies of the bonding in the Fe-Al-O system are

lacking. A quantitative comparison of the electronic interaction of the Fe cation with that of Y is not possible at this time.

2. Experimental Procedure

Samples were prepared using ultra-high purity alpha alumina powder (AKP-HP, Sumitomo Chemical Co. Osaka, Japan) for which the manufacture claims 99.995% purity. Iron and Yttrium doping was accomplished by the appropriate addition of aliquots of high purity $Fe(NO_3)_3$ (Alfa Aeser, # 10715, 99.999%) and/or $Y(NO_3)_3$ (Aldrich, #21,723-9, 99.999%) solution in deionized water to a slurry of alumina powder. After the addition of the dopant solutions, the slurry was sonically mixed until a stable suspension was produced. The suspension was then fast-frozen in liquid nitrogen and freeze-dried to ensure homogeneity. All labware contacting the powder was subjected to an acid washing procedure (see appendix). The resulting powder was calcined at 550°C in flowing oxygen for 12 hours. The powders were uni-axially pressed using a high purity alumina die and punch into pellets measuring approximately 14mm in diameter and 5mm in height. The minimal force (between 1000 and 1500 Kg depending on the powder composition) necessary to form the pellets was applied in an attempt to minimize the density gradients that arise during uniaxial pressing[9]. The pellets were then isostatically pressed at 275 MPa to a green density of approximately 50%.

The densification studies were carried out using a Lindberg model 54434 tube furnace with $MoSi_2$ heating elements. The samples were prepared under both oxidizing (flowing air) and two reducing (flowing N_2 and 96% N_2 4%H_2 mixture at 250cc/min) conditions. The oxygen partial pressure was measured to be 3.29×10^{-4} and 5.1×10^{-14} respectively

at 1350°C in the tube furnace using a type HT-600 oxygen probe from Australian Oxytrol Systems. The samples were heated at a rate of 8° C per minute to 1350° C for the indicated times and cooled at a rate of 20° C per minute. Each sample prepared in the tube furnace was embedded in a powder of identical composition in a high purity crucible (Coors Ceramic Co. #65532) to protect against furnace contamination and dopant volatilization. A different crucible was used for each powder combination. Densities were measured to an accuracy of $\pm 0.2\%$ by employing a Mettler H51 semimicro balance configured in accordance with the Archimedes method with water as the immersion medium. Grain boundaries were revealed by thermally etching the cut and polished surfaces at a temperature of 1225° C for 50 minutes (sample density < 95%) and 90 minutes (sample density > 95%).

3. The Effect Of Iron On Densification

3.1 Results

Densification curves for undoped and 1000ppm iron doped alumina in the atmospheres of air, ($Po_2 \sim 0.21$), Nitrogen, ($Po_2 \sim 3.9\times 10^{-4}$) and N_2 (96%)/H_2(4%), ($Po_2 \sim 5\times 10^{-14}$) are shown in figure 5. Curves were fitted to the densification data through the use of a log polynomial equation of the form:

$$\rho(t) = 100 - (100 - \rho_o)\exp^{f(t)} \qquad (1)$$

Here $\rho(t)$ is the percentage of the theoretical density of the sample after time t, ρ_0 is the density of the "zero" time sample and f(t) has the form of

$f(t) = A(\ln(t+1))^2 + B\ln(t+1) + C$.

The reason this form of the equation was chosen for the curve fitting is that as t approaches infinity, the density approaches a limiting value of 100%, which is the case in the system under consideration. The densification rate data acquired from equation (1) for the samples under consideration is plotted in figure 6 in the form of $\log(d\rho/dt)$ vs. the log of the grain size.

Iron at 1000ppm under oxidizing conditions reduced the densification rate by a factor of approximately 5 relative to the undoped. As the Po_2 is decreased, it can be seen that there is an increase in the densification rate for a given grain size in the iron doped samples. In the nitrogen atmosphere, the densification rate is almost identical to that of the undoped and in the N_2/H_2 atmosphere an increase of two orders of magnitude is seen over that of the undoped samples. The grain size exponents, which give an indication of the rate controlling mechanism[24], were determined by applying a linear fit to the curves of figure 6 and are presented below for the undoped and iron doped samples

Material	Grain Size Exponent
Undoped	-6.41
1000ppm Fe Air	-5.56
1000 ppm Fe Nitrogen	-4.82
1000ppm Fe N_2/H_2	-7.89

Grain size vs time curves are plotted in figure 8. Iron under oxidizing conditions was found to reduce the grain growth rate. As the Po_2 decreased, the grain growth rate increased. A plot of grain size vs. density is shown in figure 9. The trajectory (slope) of

the grain size/density curve is a measure of the ratio of the grain growth rate, $(\dot{G})$, to the densification rate, $(\dot{\rho})$, which shows that as the Po_2 is lowered, the ratio of $\dot{G}/\dot{\rho}$ is increased. Figure 7 is representative of the microstructures for all the samples for densities greater than 95% theoretical density.

3.2 Discussion of Iron Results

3.2.1 Iron Under Oxidizing Conditions

It can be seen from the density vs. time graph, figure 5, and the log $(\dot{\rho})$ vs. log (Grain Size) graph, figure 6, that iron in an oxidizing atmosphere is effective in reducing the densification rate of Al_2O_3 by a factor of approximately 5 for a given grain size when compared to the undoped samples. This may first appear to be in contradiction to previous work done by Rao and Cutler in which they found iron under oxidizing conditions to increase the volume diffusion coefficient of the oxygen, and thus the densification rate, in alumina [1]. However, due to the dissimilarities in the experimental conditions (which can be found in detail in the background section), it can be expected that a different controlling mechanism is operative. Given the experimental conditions, the effects of the dopants are more likely to manifest themselves in the grain boundaries. Therefore, we propose that the effect of iron is to hinder the grain boundary diffusion analogous to the effect of yttrium. This is entirely consistent with the creep data where a factor of 5 decrease in the strain rate was observed, Figure 1.

According to the densification models and the scaling laws of Herring [24], an indication of the rate controlling mechanism can be obtained from the slope of a plot of the log of the densification rate vs. log grain size. A slope of -3 being indicative of lattice

diffusion and a slope of -4 indicating a grain boundary controlled process. When the slopes of these curves were calculated for the undoped and the iron doped alumina under the differing atmospheric conditions, they ranged from -4.82 to -7.89 for the sample series under study. This is much larger than the predictions of the scaling laws.

This is believed to be due to the fact that the microstructures do not conform to the ideal configurations assumed by the sintering models. Specifically, the microstructures were found to exhibit some thermodynamically stable pores and a smaller number of pores per grain than the models would predict , Figure 7. Furthermore, the degree of deviation from an ideal microstructure becomes progressively more pronounced with time, explaining why the apparent grain size exponent increases correspondingly. In a similar densification study conducted by Berry and Harmer, a progressive increase in the grain size exponent was also observed as the samples reached higher densities (>95%), resulting in a slope more than -4 [9].

3.2.2 Iron Under Reducing Conditions

As can be seen from the log plot of the grain size vs. densification rate for iron doped alumina, the densification rate for a given grain size has an inverse relationship to the oxygen partial pressure. In the nitrogen atmosphere ($Po_2 \sim 3.3x\ 10^{-4}$ atm.) the densification rate for a given grain size was increased compared to iron in an oxidizing condition by a factor of approximately 5, the difference between the curves becoming more pronounced as the densification progressed. For the N_2/H_2 mix, ($Po_2 \sim 5.1 \times 10^{-14}$ atm) there was an increase of approximately 2.5 orders of magnitude. These results are consistent with prior densification studies of iron doped alumina [1,10].

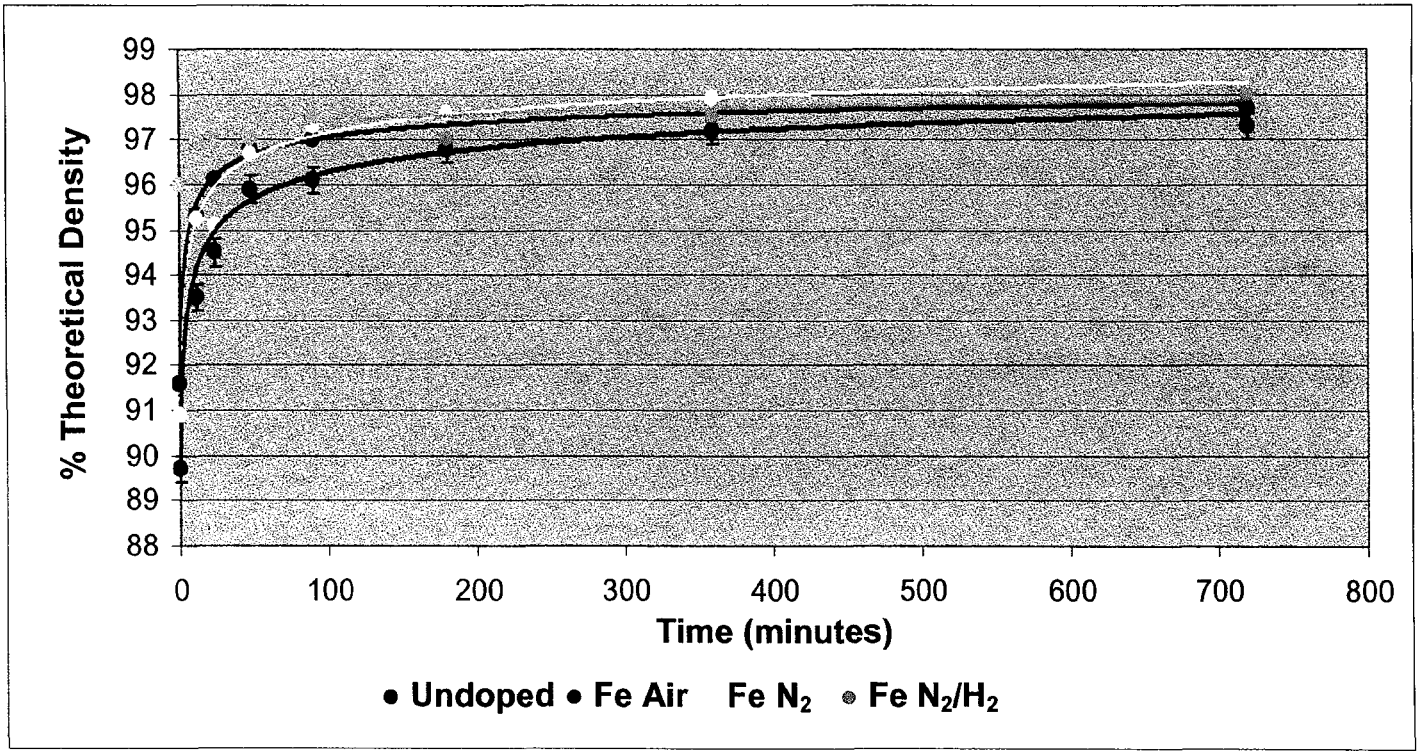

Figure 5. Density vs. time for undoped and 1000ppm Iron doped alumina densified at 1350°C in the indicated atmospheres.

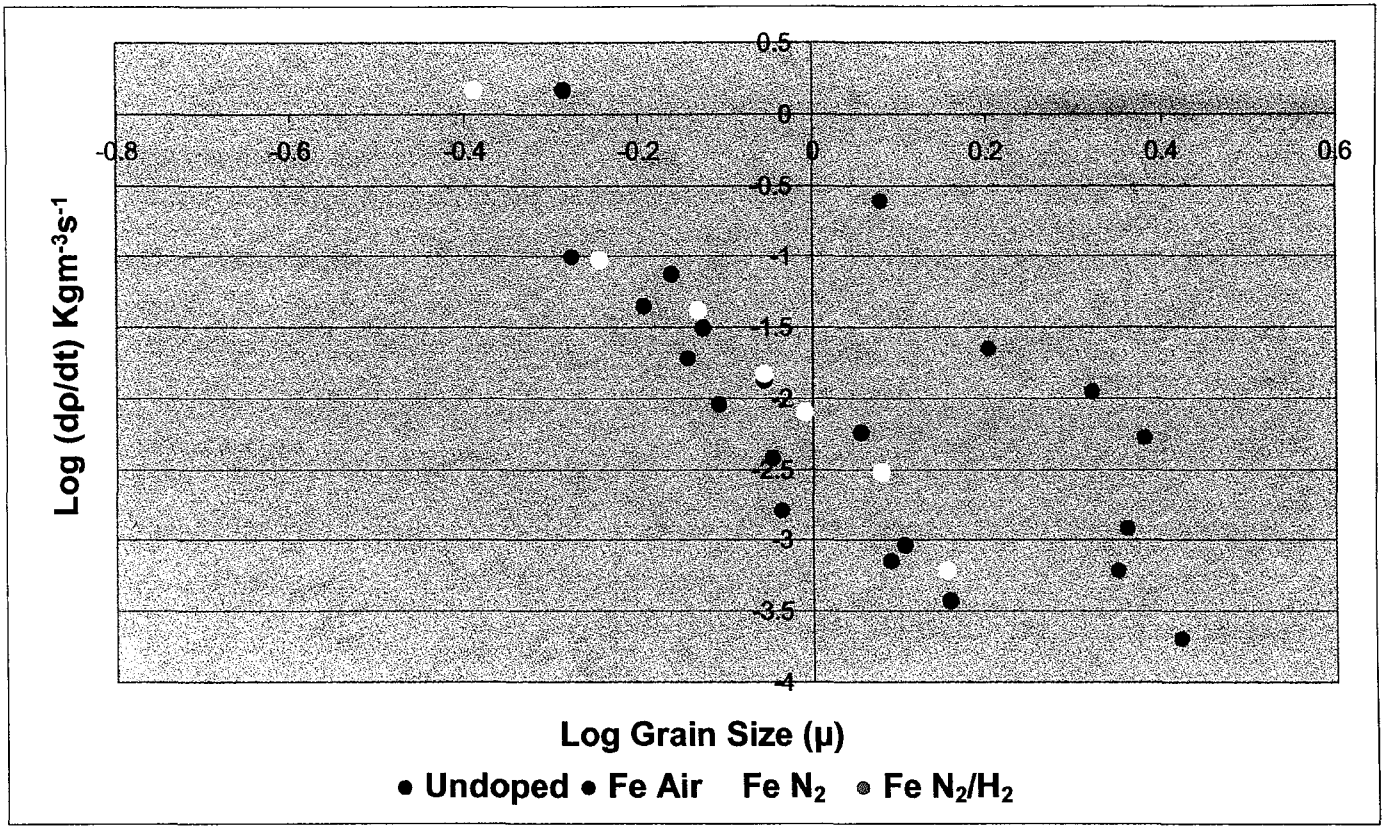

Figure 6. Log of the densification rate vs. log of the grain size showing the effect of Po_2 on the densification rate of undoped and 1000ppm iron doped alumina in the indicated atmospheres.

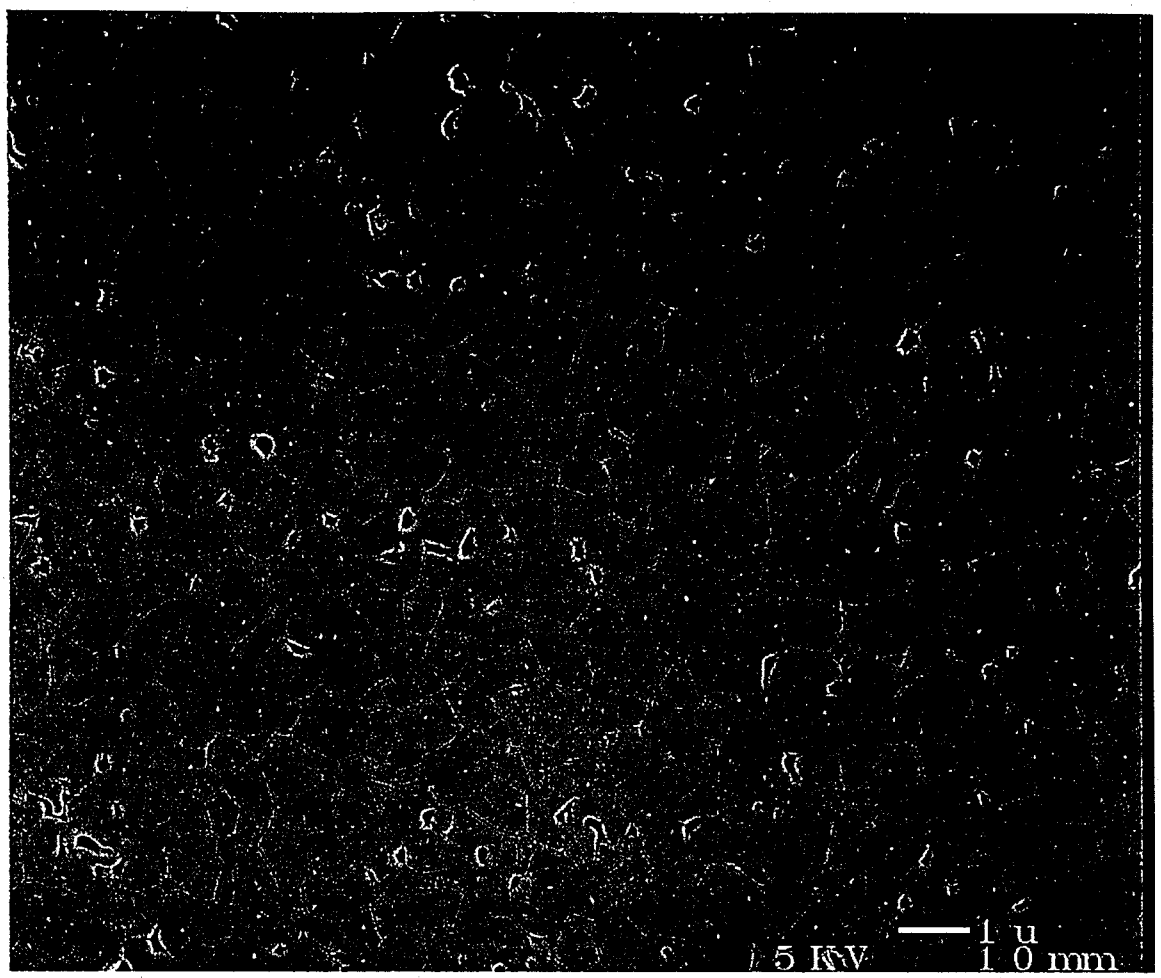

Figure 7. 1000 ppm iron doped alumina sintered to 96% density in air.

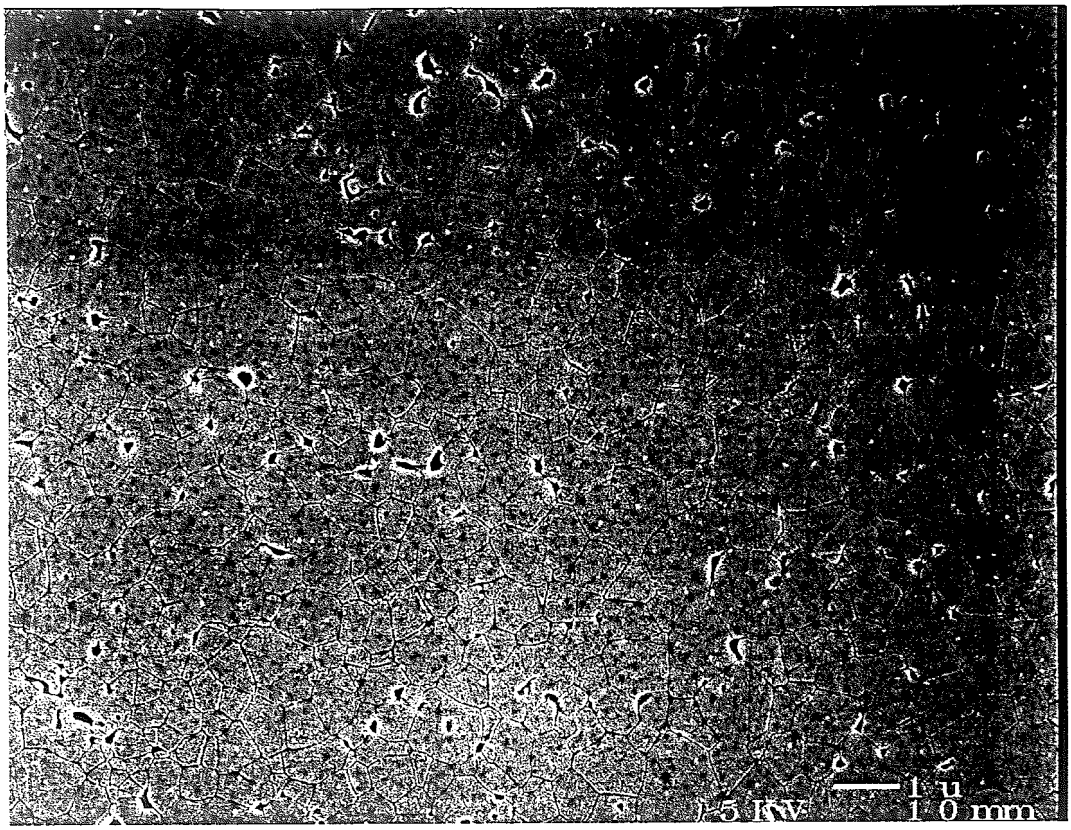

Figure 7. 1000 ppm iron doped alumina sintered to 96% density in air.

From the results of the previously mentioned research[1-5], the defect chemistry of iron in the lattice seems to be well understood. For this study however, it is the iron that is segregated to the grain boundaries that is producing the dominant effect on the densification rate of the material. This raises the question as to the role of defect chemistry in the grain boundaries. The two compensating ionic defects that can be produced are aluminum interstitials and oxygen vacancies:

$$3Fe_{Al}^{x} \Leftrightarrow 3Fe_{Al}^{'} + Al_{i}^{\cdots}$$

or

$$2Fe_{Al}^{x} \Leftrightarrow 2Fe_{Al}^{'} + V_{O}^{\cdot\cdot}$$

No previous research has examined the dominant compensating defect in the grain boundaries in this system. It is proposed that both defect types will be generated to a certain extent in the grain boundary region. Both defects are conducive to increasing the grain boundary transport rate of the material. If aluminum interstitials and oxygen vacancies are produced, it will result in the increase in the grain boundary diffusivity of aluminum and oxygen through an increase in the concentration of the mobile species. Therefore, we propose that iron promotes densification in a reducing atmosphere through the following mechanism. The concentration of Fe^{+2} is increased with decreasing Po_2. This counteracts the inhibiting effect of Fe^{+3} such that under the most reducing conditions the densification rate is enhanced.

3.3 The effect of iron on grain growth

As can be seen from the grain size vs. time and the grain size vs density graphs, figures 8 and 9, the $\dot{G}/\dot{\rho}$ is reduced by iron under oxidizing conditions but has an inverse relationship to the oxygen partial pressure in iron doped alumina. Under

oxidizing conditions, grain growth is reduced compared to that of the undoped samples. At 97% density, there is approximately a 10% difference between the average grain size of the undoped and the 1000ppm iron doped samples sintered in air. When the microstructure of the samples are examined, Figure 7, it can be seen that there are fully dense regions with stable pores interdispersed throughout the sample. This reduced grain size and lack of pores populating the grain boundary gives indication that the inhibition of grain growth is caused by a solute drag effect.

Under reducing conditions, at a density of 96%, the 1000ppm iron samples densified in air and N_2/H_2 have an average grain size of 0.75μ and 1.2μ respectively. The disparity between the two grain sizes continues to increase with continued sintering time. The observation that FeO increases the grain growth rate is consistent with the results of Zhao and Harmer [10]. In that study, an increase in the grain growth rate of 250ppm iron doped alumina compared to undoped alumina was seen under nitrogen at 1650°C.

The Cahn solute drag model is most often used to explain the effect of a solute on the grain boundary mobility, M_b,[25]. According to this model, Fe^{+2}, due to its larger size, should have more of a tendency to segregate to the grain boundaries and thus be more effective in reducing M_b than Mg^{+2}, a dopant known for its ability to reduce grain boundary mobility.

Because of the model's failure to predict the effect of Fe^{+2} on M_b, it is perhaps necessary to examine the dopants from not only a relative size perspective, but also from an electronic perspective in which the M-O bond strength is considered.

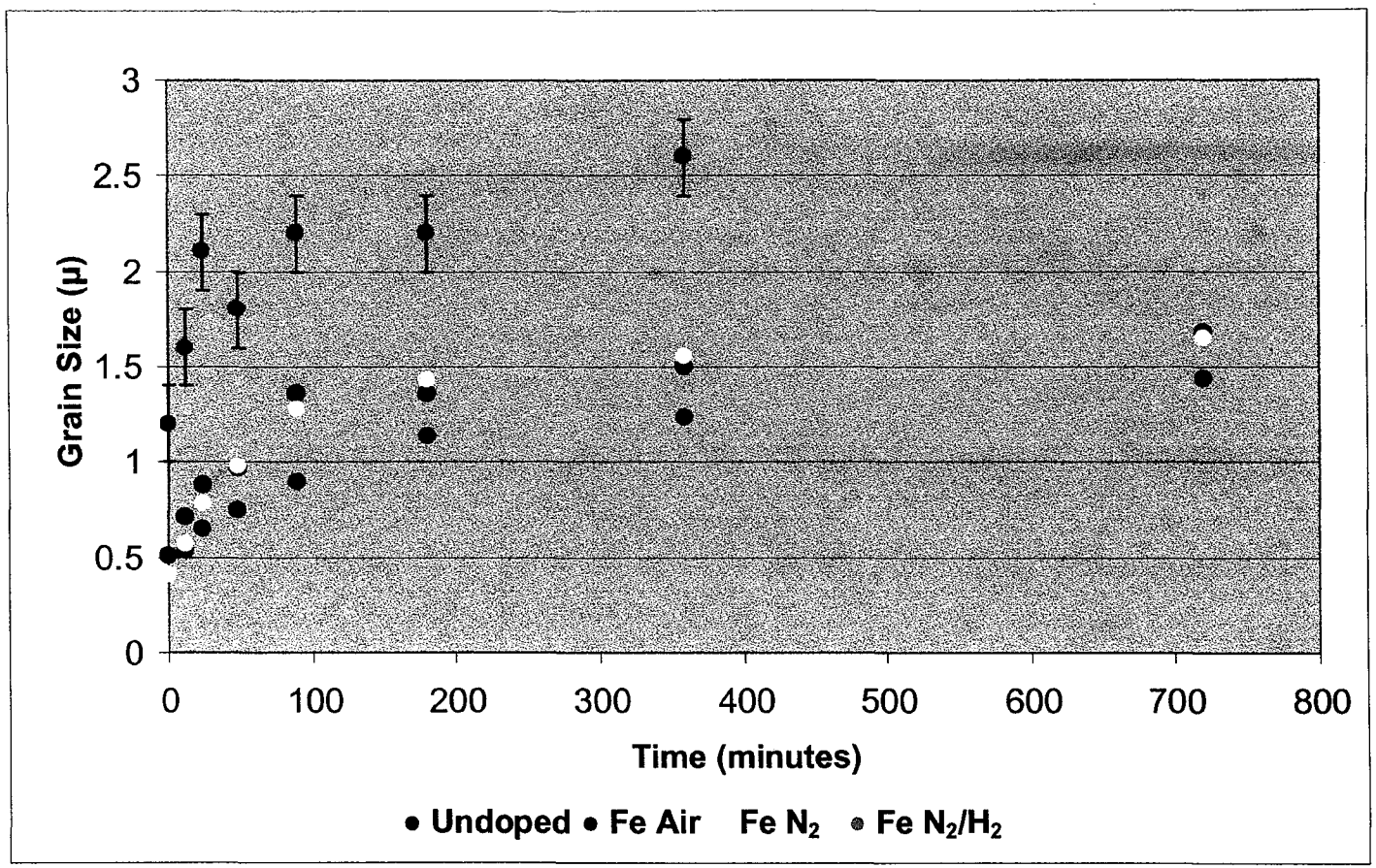

Figure 8. Grain size vs. time for undoped and 1000ppm iron doped samples densified in the indicated atmospheres at 1350°C.

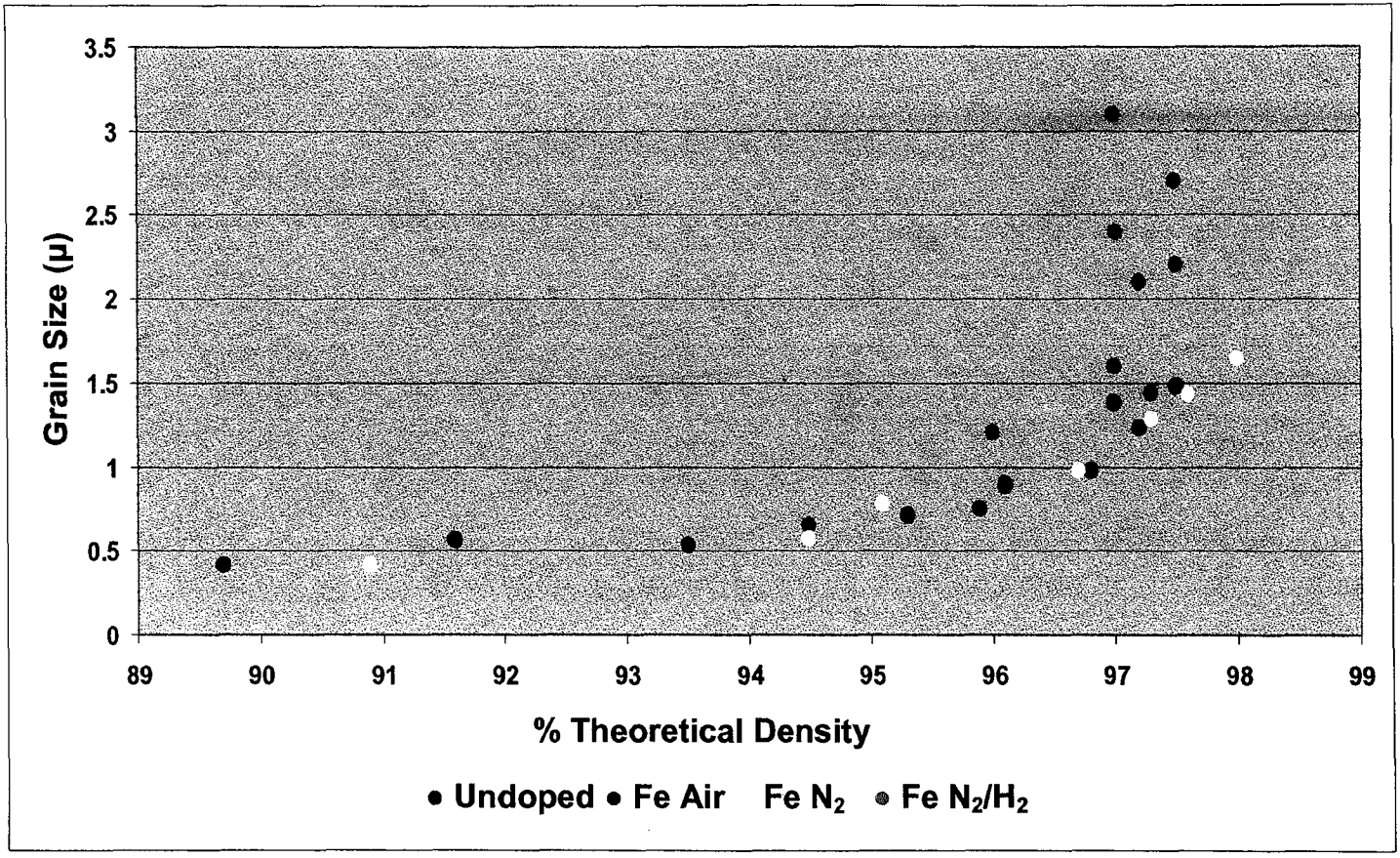

Figure 9. Grain size vs. density for undoped and 1000ppm iron doped alumina densified in the indicated atmospheres at 1350°C.

4. The Effect of Iron and Yttrium Codoping on Densification

4.1 Results

Densification curves for undoped and 1000ppm iron/yttrium codoped alumina in the atmospheres of air, ($Po_2 \sim 0.21$), Nitrogen, ($Po_2 \sim 3.9\times 10^{-4}$) and N_2H_2 ($Po_2 \sim 5\times 10^{-14}$) are shown in figure 10. The curves were fitted using the method previously described in section 2.1. It can be seen from the curves that codoping with iron to the level of this experiment does not produce any additional detectable decrease in the densification rate over the singly doped yttrium sample.

The slopes of a linear fit to the plots of log (dρ/dt) vs. log grain size of figure 11 are presented below:

Material	Grain Size Exponent
Undoped	-6.41
1000ppm Y/Fe Air	-5.25
1000ppm Y/Fe Nitrogen	-5.31
1000ppm Y/Fe N_2/H_2	-5.29

The codoping decreased the densification rate by two orders of magnitude in the early stages of sintering for the samples sintered in both air and nitrogen. This difference in densification rates decreased to one order of magnitude as the samples reached higher densities. There seemed to be no detectable difference in the sintering rates of the undoped samples and the codoped samples sintered in the N_2/H_2 atmosphere.

As with the densification rate, there was no detectable difference between the grain growth rate of the codoped samples in air and nitrogen, figure 12. The samples densified in the N_2/H_2 atmosphere displayed a reduction in grain growth relative to the undoped samples (although not as much as was present in the air and N_2 codoped samples) in the earlier stages of densification. However the difference decreased as the sintering time increased.

Examination of the plot of grain size vs. density, figure 13, shows that codoped samples sintered in air and the nitrogen atmosphere had no discernable difference in the $\dot{G}/\dot{\rho}$ ratio. As the Po_2 was lowered, there was an increase noted in the $\dot{G}/\dot{\rho}$ ratio that tended to be close to that of the undoped alumina. When the microstructure is examined, it can be seen that it is similar in configuration to that of the singly doped samples, namely fully dense areas with some thermodynamically stable pores interdispersed throughout the sample.

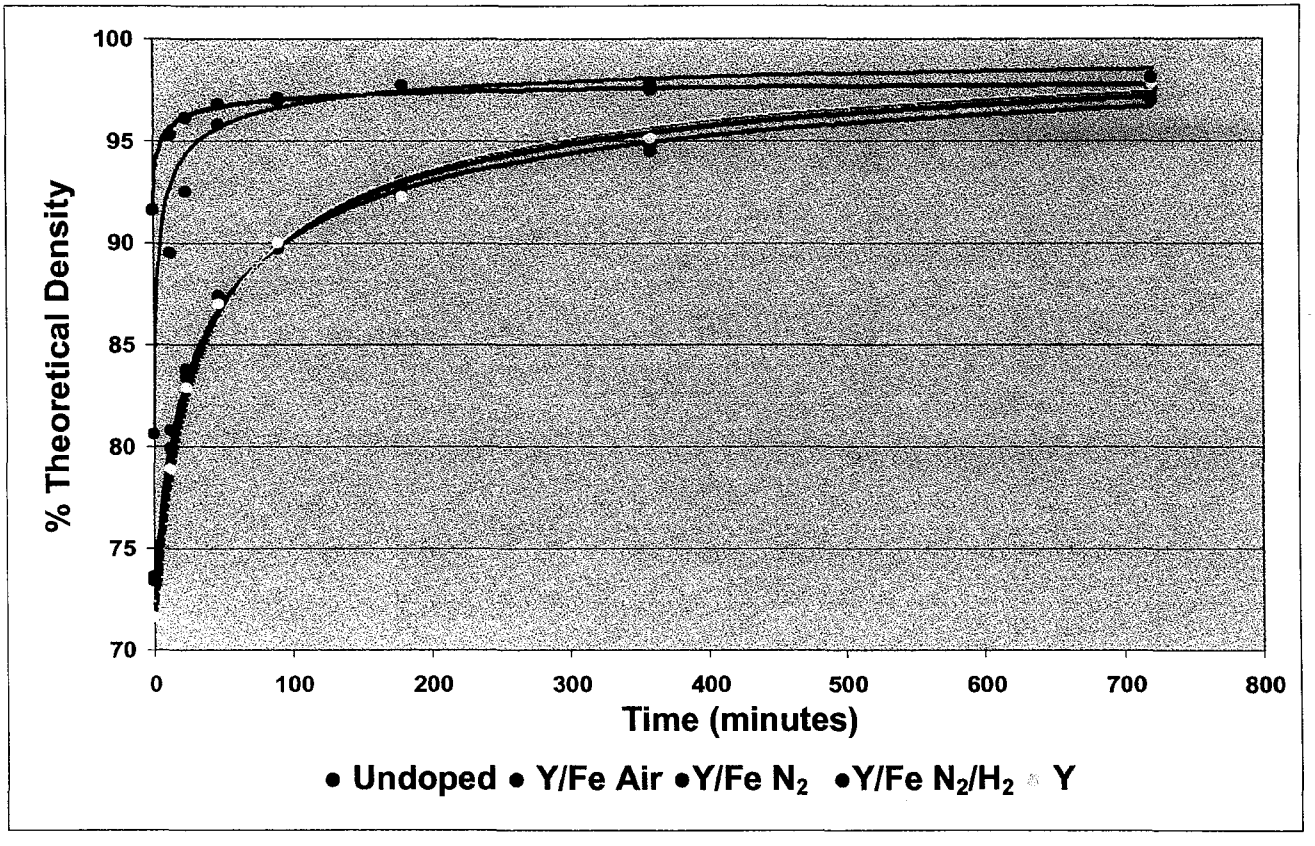

Figure 10. Density vs. time for undoped and 1000ppm iron/yttrium codoped alumina densified in the indicated atmospheres at 1350°C.

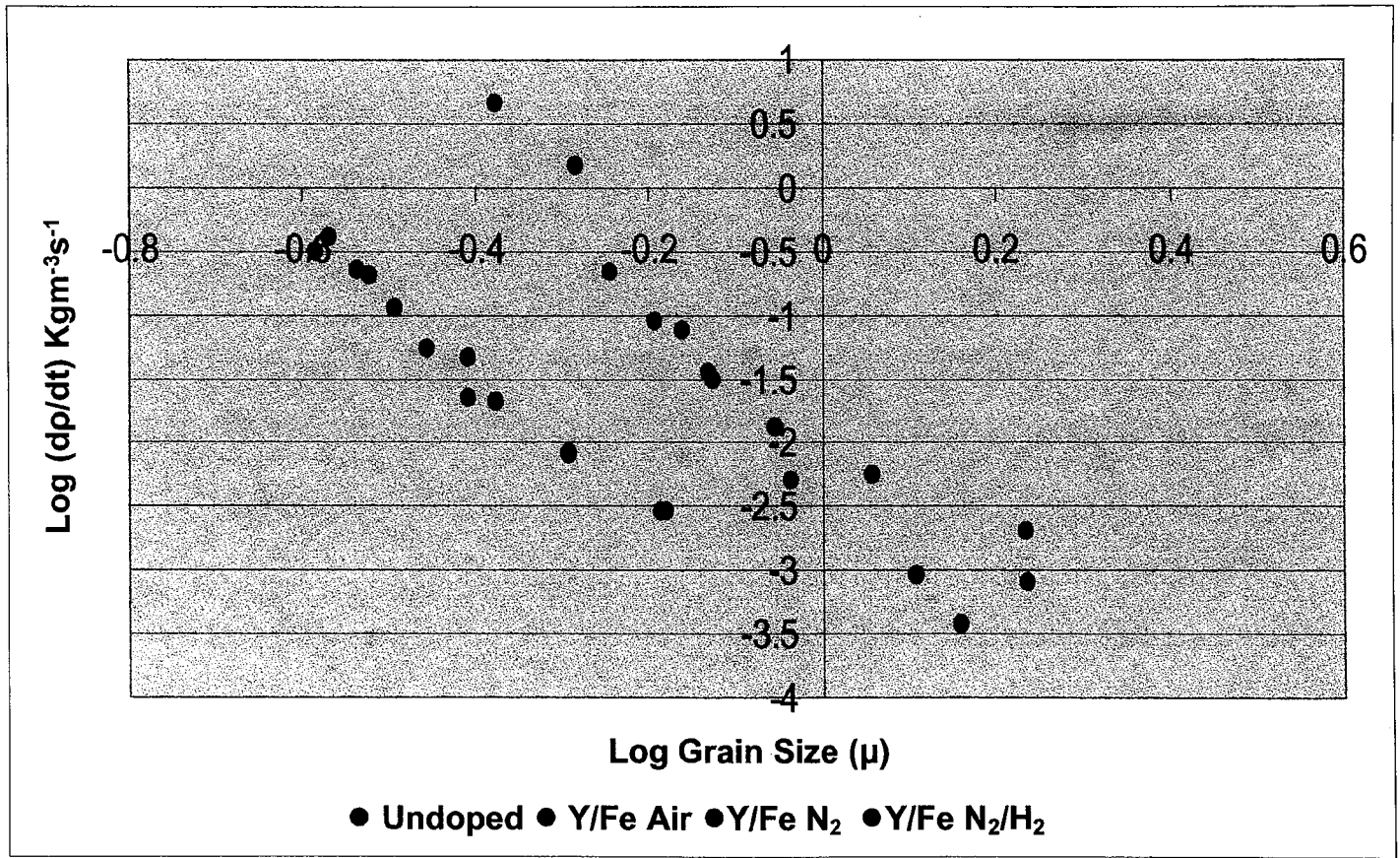

Figure 11. Log of densification rate vs log grain size for 1000ppm iron/yttrium codoped alumina densified in the indicated atmospheres at 1350°C.

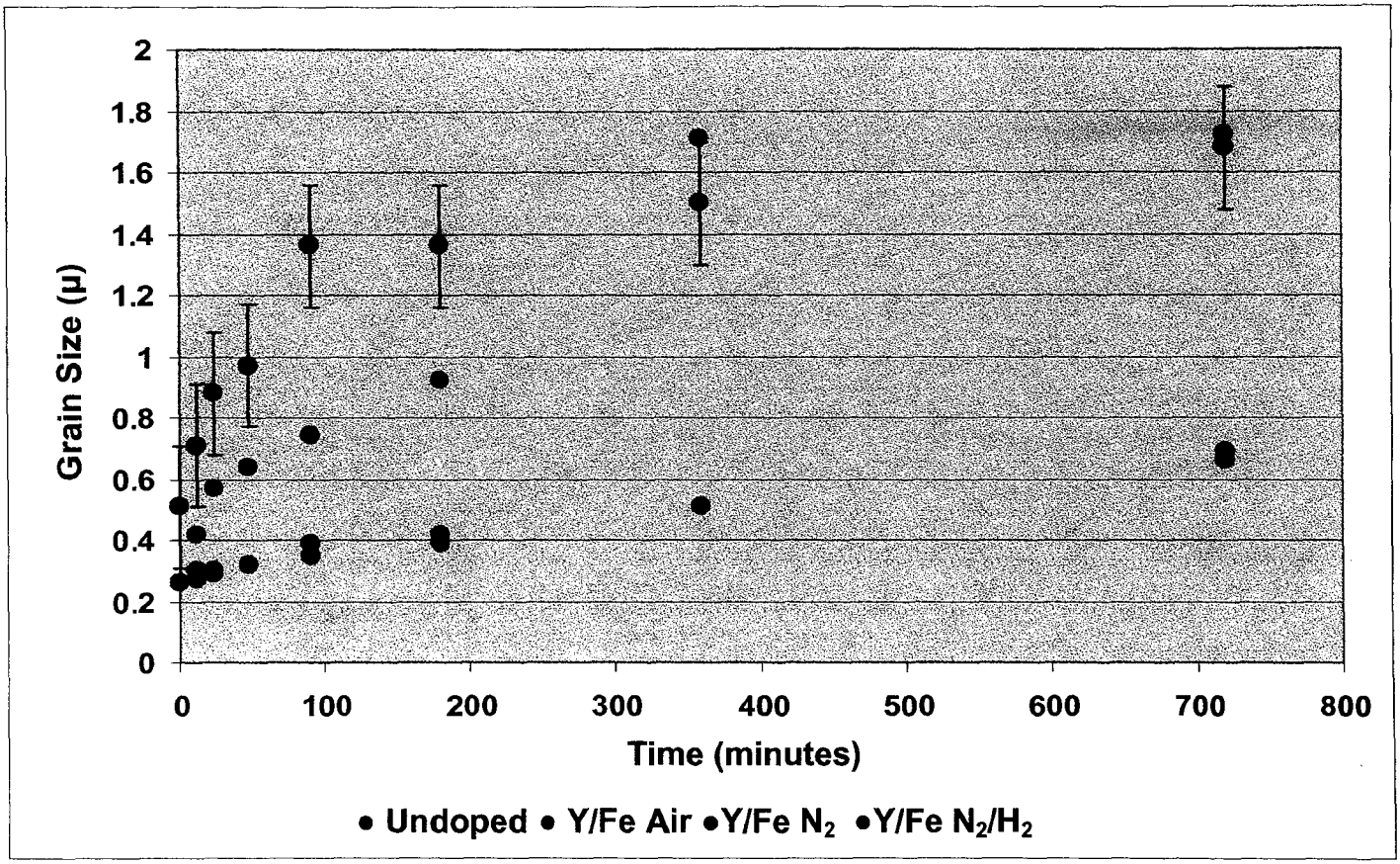

Figure 12. Grain size vs. time for undoped and 1000ppm iron/yttrium codoped alumina densified in the indicated atmospheres at 1350°C.

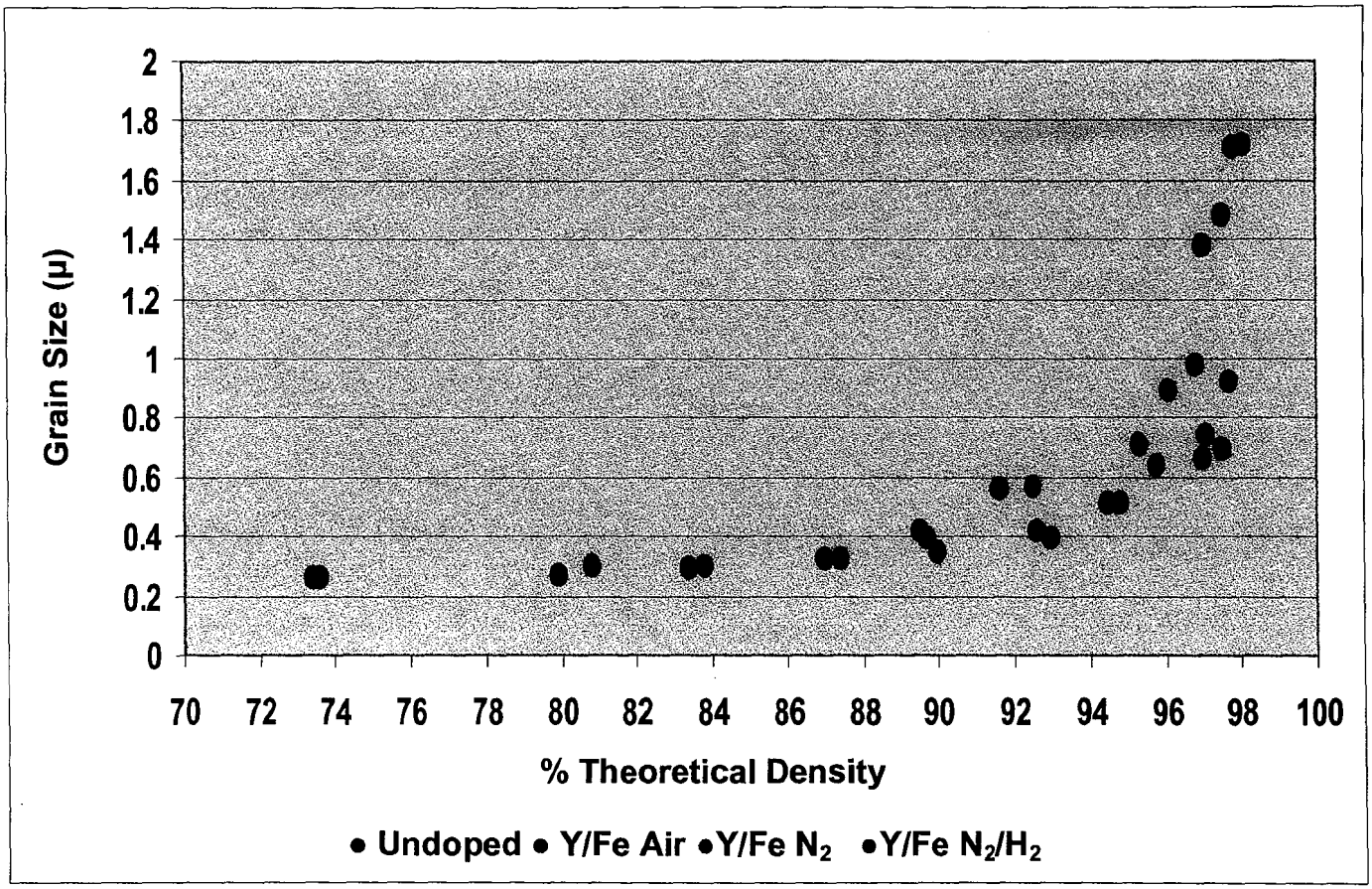

Figure 13. Grain size vs. density for undoped and 1000ppm iron/yttrium codoped alumina densified in the indicated atmospheres at 1350°C

4.2 Discussion of Codoping Results

4.2.1 Codoping under oxidizing conditions

It can be seen from figures 10 and 11, that codoping with iron and yttrium had no discernable effect in further reducing the densification rate of Al_2O_3 over that of yttrium doped alumina. One might have expected a synergistic effect, such as that observed with Nd^{+3} and Zr^{+4} codoping[26] where the Nd/Zr codoped samples had a lower creep rate than the corresponding singly doped materials. There is a 27% difference in the size of the Nd^{+3} (0.98Å) and Zr^{+4}(0.78Å) cations. The size difference would allow for more efficient filling of space in the grain boundary. This is the same percentage difference between the sizes of the Fe^{+3} (0.65Å) and the Y^{+3} (0.89Å) cations. However, the same result did not manifest itself for Fe/Y codoping. Zr^{+4} is a donor dopant in alumina and it is possible that it behaves differently due to its ability to lower the concentration of $Vo^{\bullet\bullet}$ and $Al_i^{\bullet\bullet\bullet}$.

Another factor is the limited amount of distorted sites available in the grain boundary to accommodate oversized cations. Due to its larger size and lower solubility in the lattice, yttrium is given preference over iron for the occupation of these sites. The iron, evicted from the grain boundaries, is forced to seek lodging in the near grain boundary area or deeper in the lattice. Due to the densification rate being grain boundary controlled at this grain size, the contribution of the iron will be diminished by reduced concentration in the boundaries and thus the effects of the yttrium will dominate, thus eclipsing the contribution of the iron remaining in the grain boundaries. A way to test this hypothesis

would be to measure the concentration of iron in and near the grain boundaries and in the bulk for both iron and yttrium/iron codoped samples of comparable grain size.

4.2.2 Codoping under reducing conditions

Figures 10 and 11, shows that when the Po_2 is lowered sufficiently (N_2/H_2 atmosphere) the correspondingly high Fe^{+2} concentration that is produced is sufficient to completely negate the effects of yttrium. There was no detectable difference between the codoped samples densified in an oxidizing atmosphere and those densified in a nitrogen atmosphere.

It is reasonable to postulate that the same opportunities for defect formation exist in the grain boundaries for the codoped samples as for the singly doped iron samples. Namely, that both the $Al_i^{\cdots}$ and the $V_o^{\cdot\cdot}$ can be formed as compensating point defects upon the reduction of Fe^{+3} to Fe^{+2}. In the singly doped case, it is seen that the Po_2 produced by a nitrogen atmosphere was sufficient to cause an increase in the densification rates of singly doped alumina. This was not the case in the codoped samples. We can speculate several causes for this behavior

1) The increase in bond strength caused by the presence of yttrium on both the Al cation and the O anion increase the energy of formation of the above mentioned point defects and thus hinder their formation.
2) The iron, having been partially consigned to the bulk in the competition for accommodating sites, is not as highly concentrated in the grain boundaries.

5. Conclusions

1) Fe^{+3} reduces the densification rate of fine grained alumina under oxidizing conditions consistent with recent creep data and also inhibits grain growth.
2) Fe^{+2} increases the densification and grain growth rate in fine grained alumina.
3) Y^{+3} is more effective than Fe^{+3} at reducing the densification process in alumina
4) Fe^{+2} has the ability to negate the effect of Y^{+3} on the rate processes in alumina.

References

[1] W. Rao, I. Cuttler., "Effect of Iron Oxide on the Sintering Kinetics of Al_2O_3", J. Am. Ceram. Soc., 56[11], 588-93, (1973).

[2] G. Hollenburg, R. Gordon, "Effect of Oxygen Partial Pressure on the Creep of Polycrystalline Al_2O_3 Doped with Cr, Fe, or Ti", J. Am. Ceram. Soc. 56[3], 140-47, (1973).

[3] P.A. Lessing, R. S. Gordon, "Creep of Polycrystalline Alumina, Pure and Doped With Transition Metal Impurities", J. Mater. Sci., 12, 2291-2302, (1977).

[4] B.V. Dutt, F.A. Kroger, "High-Temperature Defect Structure of Iron Doped α-Alumina" J. Am. Ceram. Soc.,58[12] 474-76, (1975).

[5] Y. Ikuma, R.S. Gordon, "Effect of Doping Simultaneously with Iron and Titanium on the Diffusional Creep of Polycrystalline Al_2O_3" J. Am. Ceram. Soc., 66[2], 139-147, (1983).

[6] J. F. Laurent, J. Benard, "Self-Diffusion of Ions in Polycrystalline Alkali Halides", Phys. Chem. Solids, 7[2-3], 218-27, (1958).

[7] W. S. Young, I.B. Cutler, "Initial Sintering With Constant Rates Of Heating", J. Amer. Ceram. Soc., 53[12], 659-63,(1970).

[8] Y. Ikuma, R.S. Gordon, "Enhancement of diffusional creep of polycrystalline Al_2O_3 by simultaneous doping with manganese and titanium", J. Mater. Sci. 17, 2961-67, (1982).

[9] K. A. Berry, M. P. Harmer, "Effect of MgO Solute on Microstructure Development of Al_2O_3." J. Am. Ceram. Soc. 69[2], 143-49, (1986).

[10] J. Zhao, M.P. Harmer, "Sintering of Ultra-High-Purity Alumina Doped Simultaneously with MgO and FeO", J. Am. Ceram. Soc., 70[12], 860-66, (1987).

[11] J. D. French, J. Zhao, M. P. Harmer, H. M. Chan, G. A. Miller, "Creep of Duplex Microstructures" J. Am, Ceram. Soc. 77[11], 2857-65, (1994).

[12] J. Cho, M. P. Harmer, H. M. Chan, J. M. Rickman, A. M. Thompson, "Effect of Yttrium and Lanthanum on the Tensile Creep Behavior of Aluminum Oxide", J. Am. Ceram. Soc. 80[4], 1013-17, (1997).

[13] H. Yoshida, I. Ikuhara, T. Sakuma, "High Temperature Creep Resistance In Rare Earth Doped Fine-Grained Alumina", J. Mater. Res., 13[9], 2597-2601, (1998).

[14] S. Lartigue-Korinek, C. Carry, L. Priester, "Multiscale aspects of the influence of yttrium on microstructure, sintering and creep of alumina", J. Eur. Ceram. Soc., 22,[9-10],1525-1541, (2002).

[15] D. Prott, M. Le Gall, B. Lesage, A.M. Huntz, C.Monty "Self-Diffusion in α-Al_2O_3 IV. Oxygen Grain-Boundary Self-Diffusion in Undoped and Yttria-Doped Alumina Polycrystals", Philos. Mag. A, 73[4], 935-949, (1996).

[16] P. Gruffel, C. Carry, "Effect of Grain Size on Yttrium Grain Boundary Segregation in Fine-Grained Alumina", J. Eur. Ceram. Soc. 11, 189-199, (1993).

[17] J. Fang, A. M. Thompson, M. P. Harmer, H. M. Chan, "Effect of Yttrium and Lanthanum on the Final Stage Sintering Behavior of Ultrahigh-Purity Alumina", J. Am. Ceram. Soc., 80[8], 2005-12,(1997).

[18] S. Fabris, C. Elsasser, "First-Principals Analysis of Cation Segregation at Boundaries in α-Al_2O_3" Acta Mater., 51, 71-86, (2003).

[19] C. Elsasser, A.G. Marinopoulous, "Substutional Cation Impurities in α-Al_2O_3: Ab-Initio Case Study Of Segregation To The Rhombohedral Twin Boundary" Acta Mater., 49, 2951-2959, (2001).

[20] P. R. Kenway, "Calculated Structures and Energies of Grain Boundaries in α-Al_2O_3," J. Am. Ceram. Soc., 77[2], 349-55 (1994).

[21] S. D. Mo, W. Y. Ching, "Electronic Structure of a Near $\Sigma 11$ *a*-axis Tilt Grain Boundary in α-Al_2O_3," J. Am. Ceram. Soc., 79, 627-33 (1996).

[22] K. Kaneko, T. Gemming, I. Tanaka, H. Mullejans, "Analytical Investigation of Random Grain Boundaries of Zr-Doped Sintered α-Al_2O_3 by Transmission Electron Microscopy and Scanning Transmission Electron Microscopy," Philos. Mag. *A*, 77, 1255-72 (1998).

[23] W. Y. Ching, Y. N. Xu, "Nonscalability and Nontransferability in the Electronic Properties of the Y-Al-O System," Phys. Rev. B, 59, 12815-21 (1999).

[24] Herring, C."Effect of Change of Scale on Sintering Phenomena ", J. App. Phys. 21, 301-06, (1950).

[25] J.W. Cahn, "Impurity Drag Effect On Grain Boundary Motion", Acta Metall., 10(9) 355-78 (1968).

[26] Y. Li, C. Wang, H.M. Chan, J.M.Rickman, M.P. Harmer, "Codoping of Alumina to Enhance Creep Resistance", J. Am. Ceram. Soc., 82 (6), 1497-504 (1999).

Appendix

Acid Washing Procedure:

Materials needed:

1) Trichloroethylene
2) Acetone
3) Ethanol
4) Deionized Water
5) Nitric Acid
6) Hydrochloric Acid
7) Hydrofluoric Acid

The purpose of acid washing the labware is to remove organic, metallic and glass contaminants. All procedures should be done in a fume hood. Please note the hazards of hydrofluoric acid and exercise the necessary cautions in its handling.

1) Place the object being washed in an appropriate container that is chemically resistant to the substances it will come in contact with.
2) Pour enough Trichloroethylene into the washing container to cover the object(s) being washed; close the lid and shake for one minute and then let stand for ten minutes.
3) The trichloroethylene may be recycled and used over if it is not contaminated. Pour it into the appropriately labeled container for reuse or disposal.
4) Refill the washing container with acetone, shake for one minute, let stand for ten minutes.
5) The acetone can not be recycled, pour it into an appropriately labeled container for disposal.
6) Refill the washing container with ethanol, shake for one minute and let stand for ten minutes.
7) Dispose of the ethanol by pouring it down the drain with the cold water running. Triple rinse the contents of the washing container with deionized water.
8) Add one part Nitric acid to three parts Hydrochloric acid to the washing container. This is a mixture known as "Aqua Regia" and is used for its oxidative powers to remove metal contamination. The mixture will turn orange and begin to bubble. The bubbles are oxides of nitrogen. DO NOT CLOSE THE LID ON THIS MIXTURE. Allow it to stand for one hour.
9) Pour the Aqua Regia into an appropriate container for storage/ disposal and triple rinse the contents of the washing container with deionized water.

All ceramic labware is finished at this point. Hydrofluoric acid will etch ceramics.

10) Make a 5:1 mixture of deionized water to hydrofluoric acid in the washing container. **POUR THE DEIONIZED WATER IN FIRST. NEVER ADD WATER TO ACID...ALWAYS ADD ACID TO WATER. REMEMBER "AA"..."ADD ACID".** Let the mixture stand for one hour and the triple rinse with deionized water.
11) Remove the acid washed labware to the clean room for drying.

VITA

Michael David Drahus was born on March 21, 1965 in the city of Scranton, PA. to Michael and Helen Drahus of 712 Birch St. Moscow, PA. He attended North Pocono High School for his secondary education. After graduating in 1983, he departed for Fort Knox, Kentucky to begin basic training for his enlistment in the U.S. Army as a tanker. He was stationed in Bad Hersfeld, Germany until 1986 when he was discharged. He then returned to the Scranton area and began working in the construction field.

An interest in science soon became a motivating factor to return to school and he attended Penn State University where he received an associates degree in Letters, Arts and Sciences. These credits were then applied to a Bachelors degree in Physics with a Chemistry minor at the University of Scranton. At the time, he was self-employed performing restoration work on the older houses in the Scranton area.

He enrolled in Lehigh University in Janurary of 2000 where he has spent many enjoyable hours learning the use of new lab equipment and experimental and analytical techniques. He is a member of the American Ceramics Society.

What's next? That chapter has yet to be written.

END OF TITLE